
Research Article: New Research | Sensory and Motor Systems

The G-protein coupled receptor SRX-97 is required for concentration dependent sensing of benzaldehyde in *Caenorhabditis elegans*

<https://doi.org/10.1523/ENEURO.0011-20.2020>

Cite as: eNeuro 2021; 10.1523/ENEURO.0011-20.2020

Received: 9 January 2020

Revised: 16 December 2020

Accepted: 18 December 2020

This Early Release article has been peer-reviewed and accepted, but has not been through the composition and copyediting processes. The final version may differ slightly in style or formatting and will contain links to any extended data.

Alerts: Sign up at www.eneuro.org/alerts to receive customized email alerts when the fully formatted version of this article is published.

Copyright © 2021 Kadam et al.

This is an open-access article distributed under the terms of the Creative Commons Attribution 4.0 International license, which permits unrestricted use, distribution and reproduction in any medium provided that the original work is properly attributed.

1 **Title Page**

2

3 **Title:**

4 The G-protein coupled receptor SRX-97 is required for concentration dependent
5 sensing of benzaldehyde in *Caenorhabditis elegans*

6

7 **Running title:**

8 SRX-97 receptor is required for sensing benzaldehyde

9

10 **Author List:**

11 Nagesh Y. Kadam^{1,4}, Sukanta Behera¹, Sandeep Kumar³, Anindya Ghosh-Roy³ and
12 Kavita Babu^{1,2,4}

13

14 **Author Affiliations:**

15 1. Department of Biological Sciences, Indian Institute of Science Education and
16 Research (IISER) Mohali, Knowledge City, Sector 81, SAS Nagar, Manauli PO
17 140306, Punjab, India.

18 2. Centre for Neuroscience, Indian Institute of Science, CV Raman Road, Bangalore
19 560012, Karnataka, India.

20 3. National Brain Research Centre, Manesar, Nainwal Mode, Gurgaon 122051, Haryana,
21 India.

22

23 4. Corresponding author: Kavita Babu (kavita.babu@babulab.org or kavitababu@iisc.ac.in)
24 and Nagesh Kadam (nagesh.kadam@babulab.org)

25

26

27

28 **Keywords:** SRX-97, ASH neuron, Benzaldehyde and *C. elegans*

29

30

31

32 **Abstract**

33 The G-protein (heterotrimeric guanine nucleotide-binding protein)-coupled receptors in
34 the olfactory system function to sense the surrounding environment and respond to
35 various odorants. The genes coding for olfactory receptors in *Caenorhabditis elegans*
36 are larger in number in comparison to those in mammals, suggesting complexity in the
37 receptor-odorant relationships. Recent studies have shown that the same odorant in
38 different concentrations could act on multiple receptors in different neurons to induce
39 attractive or repulsive responses. The ASH neurons are known to be responsible for
40 responding to high concentrations of volatile odorants. Here we characterize a new
41 GPCR, SRX-97. We found that the *srx-97* promoter drives expression specifically in the
42 head ASH and tail PHB chemosensory neurons of *C. elegans*. Moreover, the SRX-97
43 protein localizes to the ciliary ends of the ASH neurons. Analysis of CRISPR-based
44 deletion mutants of the *srx-97* locus suggests that this gene is involved in recognition of
45 high concentrations of benzaldehyde. This was further confirmed through rescue and
46 neuronal ablation experiments. Our work brings novel insights into concentration-
47 dependent receptor function in the olfactory system, and provides details of an
48 additional molecule that helps the animal navigate its surroundings.

49

50 **Significance Statement**

51 Although GPCRs have been known to function as chemosensory receptors, the
52 expression pattern and function of a large number of GPCRs remains unknown. This
53 work sheds light on the expression pattern of an uncharacterized GPCR, SRX-97. Our
54 work shows that this protein is expressed very specifically in two sensory neuron pairs
55 in the head and tail region and is required for concentration dependent sensing of odors
56 in *C. elegans*.

57 **Introduction**

58 Animals sense a wide range of volatile and water-soluble chemicals through their
59 olfactory system. The olfactory system consists of several neurons that express
60 different sets of seven-transmembrane G-protein coupled receptors (GPCRs). The
61 odorant binds to the GPCRs, activating distinct intracellular signaling pathways and thus
62 directing the animal's response to different external cues (reviewed in (Erlandson et al.,
63 2018; Katritch et al., 2013)).

64 *Caenorhabditis elegans* are soil-dwelling animals that possess well-developed
65 chemosensory systems for their survival. They perceive their environment through
66 various sensory neurons to find food sources, mates, and to escape from dangerous
67 conditions. In *C. elegans*, 13 pairs of chemosensory neurons carry out the majority of
68 chemosensation as they express around 1300 functional chemosensory (cs) G-protein
69 coupled receptors (GPCR) (Robertson and Thomas, 2006; Vidal et al., 2018). This
70 diversity of csGPCRs allows the animal to discriminate between different odors. Thus,
71 the specific expression of any GPCR or combined expression of different GPCRs on a
72 specific neuron or in multiple neurons can modulate the animal's perception towards the
73 same odorant.

74 The olfactory neurons that are involved in sensing a large number of attractive cues are
75 the AWA and AWC neurons. These two pairs of neurons are involved in chemotaxis to
76 various chemicals like diacetyl, isoamyl alcohol, pyrazine, benzaldehyde, and butanone
77 (Bargmann et al., 1993; Colbert et al., 1997; Troemel et al., 1995). The avoidance
78 behavior towards the repellents nonanone and 1-octanol is mediated through the
79 sensory neurons AWB, ASH, and ADL (Chao et al., 2004; Troemel et al., 1997).

80 Besides this, many volatile chemicals detected by olfactory neurons could act as
81 attractants at low concentrations and repellents at high concentrations (Yoshida et al.,
82 2012). For example, at low concentrations diacetyl is sensed by the GPCR ODR-10, in
83 the AWA neuron acting as an attractant (Sengupta et al., 1996), whereas at high
84 concentration it is sensed by the SRI-14 GPCR in the ASH neurons and acts as a
85 repellent (Taniguchi et al., 2014). Additionally, ASH neurons are polymodal neurons
86 involved in avoidance behaviors towards different nociceptive signals, like noxious
87 chemicals, nose touch, hyperosmolarity, and volatile repellents (Bargmann, 2006;
88 Hilliard et al., 2005). The ASH neurons convey information through multiple receptors.
89 For example, nose touch has been shown to be detected by TRP (transient receptor
90 potential) channel proteins like OSM-9 and OCR-2 (Colbert et al., 1997; Tobin et al.,
91 2002), while hyperosmolarity is detected by OSM-10 (Hart et al., 1999). The ASH
92 neurons forms strong synaptic connections with the AVA command interneurons, which
93 regulates the backward locomotion of *C. elegans* (Bhardwaj et al., 2020; Bhardwaj et
94 al., 2018; Gray et al., 2005; Pokala et al., 2014; Zheng et al., 2012). Thus, activation of
95 ASH neurons can affect backward locomotion or avoidance behaviors in *C. elegans*.

96 ASH neurons are also reported to be involved in sensing undiluted or high
97 concentrations of benzaldehyde (Aoki et al., 2011; Taniguchi et al., 2014; Troemel et al.,
98 1995; Walker et al., 2009). Here, we show that SRX-97 is expressed in the ASH
99 neurons. We have used the CRISPR/Cas9 method for genome editing and have made
100 a deletion in the *srx-97* gene locus, generating a null mutation in *srx-97*. The *srx-97*
101 mutants present defects in chemotaxis behavior, more specifically towards high
102 concentrations of benzaldehyde. Moreover, the mutant phenotype could be rescued by

103 both endogenous and neuron-specific expression of the wild-type *srx-97* gene,
104 suggesting concentration-dependent behavioral plasticity for odors in *C. elegans*
105 through the SRX-97 GPCR.

106

107 **Materials and Methods**

108 ***C. elegans* strains and maintenance**

109 All *C. elegans* strains were maintained on nematode agar growth media (NGM) plates
110 seeded with OP50 *Escherichia coli* at 20 °C under standard conditions (Brenner, 1974).
111 The *C. elegans*, N2 (Bristol strain) was used as the wild-type (WT) control, and the
112 mutant strains CX2205 *odr-3* (*n2150*) V, CX10 *osm-9* (*ky10*) IV, NL792 *gpc-1(pk298)* X,
113 RB2464 *tax-2* (*ok3403*) I and VC3113 *tax-4* (*ok3771*) III, as well as the AWC ablated
114 strain PY7502 *oyls85* (*Pceh-36::TU#813* + *Pceh-36::TU#814* + *Psrtx-1::GFP* + *Punc-*
115 *122::DsRed*, TU#813 and TU#814 are split caspase vectors) used in this study were
116 obtained from the *Caenorhabditis* Genetic Centre (CGC). Double mutants were made
117 through standard genetic procedures and verified using PCR. The list of primers used
118 for PCR verification in this study is tabulated in Table 1. The strains used in this study
119 are listed in Table 2.

120 **Rescue constructs and transgenes**

121 All constructs for the rescue of the *srx-97* phenotype were generated using standard
122 cloning methods (Russell, 2001). The *pPD49.26* and *pPD95.75* vectors were used to
123 clone the constructs. The primers used for cloning are indicated in Table 1. The
124 transgenic strains were generated using standard microinjection techniques as
125 described previously (Mello and Fire, 1995; Mello et al., 1991). The *pCFJ90* and

126 *pPD95.75* plasmids were used to amplify or clone mCherry and GFP, respectively. The
127 rescue constructs or promoter fusion constructs were injected at 20-30 ng/μl. *Pmyo-*
128 *2::mCherry* (2 ng/μl) or *Punc-122::GFP* (25 ng/μl) were used as co-injection markers.
129 The constructs used in this study are described in Table 3.

130 **Imaging experiments**

131 Young adult animals were used for imaging. The animals were immobilized with 30
132 mg/ml 2, 3-butanedione monoxamine (BDM) on 2% agarose pads in M9 media. The
133 promoter mCherry images for ASH and PHB were acquired on a Leica SP6 upright
134 laser scanning confocal microscope using the 40X oil-immersion objective lens. Laser
135 lines from He-Ne (594) with HyD detectors were used to image fluorescence in the head
136 and tail regions. All other imaging experiments were performed with oil immersion
137 40X/1.4, 63X/1.4 or 100X/1.4 plan Achromat objectives using a Zeiss AxioCam MRm
138 CCD camera on the Zeiss AxioImager Z2 microscope.

139 **Behavioral assays**

140 Chemotaxis assay

141 The chemotaxis assay was performed using young adult *C. elegans*. Young adult
142 animals were obtained by bleaching gravid adults and incubating the remaining eggs for
143 72 hours (h) at 20 °C. All chemotaxis assays were performed with standard 90 mm
144 petriplates containing 15-18 ml of chemotaxis medium (Agar, MgSO₄ (1 M) CaCl₂ (1 M)
145 and KPO₄ (1 M) at pH 6.6). Wherever required, odorants were diluted in ethanol and
146 reported as a percent by volume. Modified 90 mm quadrant plate chemotaxis assays
147 were performed as described previously (Bargmann et al., 1993; Margie et al., 2013).
148 Briefly, 5 minutes (min) prior to the assay, 1 μl of 0.5 M sodium azide was applied on

149 four spots that were each 3 cm from the loading center. Sodium azide acts as an
150 anesthetic agent to immobilize animals that reach the vicinity of the spot during the
151 assay. 50-150 animals were placed at the center of the plate between the four spots, 2
152 μ l of ethanol were placed at the two-control spots and 2 μ l of the test odorant were
153 placed at the two-test spots. After 90 min of chemotaxis, animals within each sector
154 were counted, and the Chemotaxis Index (C.I.) was calculated as the number of
155 animals in the two test sectors minus the number of animals in the two control sectors,
156 divided by the total number of animals on the plate excluding those that were not
157 moving at the center of the plate (illustrated in Figure 3-1A). A positive C.I. indicates an
158 attraction to the chemical, and a negative C.I. indicates a repulsion to the chemical.

159 Assay to evaluate chemotaxis frequency

160 For analysis of the frequency or number of animals chemotaxing towards the source of
161 benzaldehyde, a modified grid chemotaxis plate was used (Nuttley et al., 2001). The
162 sodium azide was omitted so that animals could leave a spots after an initial approach.
163 This grid consisted of four parallel lines drawn 1 cm apart to divide the plate area into
164 five sectors, with the distance between the second and third lines being 2 cm (illustrated
165 in Figure 4A). Two microliters of benzaldehyde were placed on one small sheet of
166 parafilm, and the same amount of ethanol was placed on another as a control. The
167 benzaldehyde and ethanol were placed at opposite ends of the plate (6 cm away). After
168 a 60 min time interval, animals were immobilized by cooling the plates for 3 min at -30
169 $^{\circ}\text{C}$, and the plates were maintained at 4°C until counting. The number of animals in
170 sectors a–d, with the test odorant being in a and d, were counted and the kinetic C.I.
171 was calculated as (no. of animals in a + no. of animals in b) – (no. of animals in c + no.

172 of animals in d) / (total number of animals on the plate), yielding a C.I. range between
173 +1.0 and -1.0 (illustrated in Figure 4A). The animals that had crawled up the sides of
174 the plate were excluded from the analysis. The score of 50–150 animals for each plate
175 was used as one data point.

176 Dry drop avoidance assay

177 A drop of a solution containing the test chemicals (SDS, quinine, CuSO₄, glycerol, and
178 dihydrocaffeic acid) dissolved in M13 buffer (Tris, 30 mM; NaCl, 100 mM; KCl, 10 mM)
179 was delivered on the agar plate (NGM unseeded) 0.5-1 mm anterior to the moving
180 animals (Hilliard et al., 2002). Once the animal encountered the dry drop of chemical,
181 the head amphid neurons sensed the chemical triggered repulsion/avoidance behavior.
182 The delayed response in seconds (sec) from the initial contact to a reversal was
183 calculated in the assay. Videos were recorded for 1 min at 10 frames/sec with 1-2
184 readings leaving a gap of 20-30 sec between each trial. The graphs were plotted by
185 taking the average value from 2 trials with more than 30 animals being analyzed for
186 each condition over multiple days. If the animal failed to respond within 6 sec, the
187 reversal time was considered as 6 sec. Drops of M13 buffer were used as a control
188 where animals as expected did not show robust responses (Table 5). Glass capillaries
189 (10 mm) pulled by hand on flames to reduce the diameter of the tip were used to deliver
190 the drops. The results were plotted using GraphPad Prism V6 and evaluated using One-
191 Way ANOVA. The mean \pm SEM were plotted.

192 Nose touch assay

193 The response to nose touch was analyzed on unseeded plates as described previously
194 (Kaplan and Horvitz, 1993). Briefly, young adult animals were placed on NGM plates

195 and allowed to habituate for 1 min. An eyelash was placed in the path of the forward
196 moving animal, and those who showed a reversal of the body movement upon collision
197 with the eyelash were considered as positive responders. The experiment was
198 performed with 20-30 animals per genotype over multiple days. The analysis was
199 performed using 10 trials/ animal, and the data is shown as the percentage of positive
200 responders.

201 Aldicarb assay

202 The aldicarb assays were performed as described previously (Mahoney et al., 2006).
203 Briefly, Aldicarb plates were made the previous day by adding 100 mM stock solution
204 (prepared in ethanol) of aldicarb (Sigma-Aldrich, USA) to molten NGM at a final
205 concentration of 1 mM. Plates were then seeded with OP50 *E. coli* and stored in dark at
206 room temperature overnight. For each assay 20-25 young adult animals were
207 transferred on to the aldicarb plates and scored for paralysis every 10 min for upto 120
208 min. Animals were considered paralyzed when they failed to show body bends following
209 prodding three times on the head.

210 **Ablation of ASH neurons**

211 ASH neuronal ablation experiments were performed to test the benzaldehyde
212 chemotaxis dependence on this neuron, which was tagged with *Psrx-97::mCherry*. L2
213 staged animals were used for the ablation experiment, as ablations are more effective in
214 early stages (Avery and Horvitz, 1987, 1989; Bargmann and Horvitz, 1991). During
215 ablation and imaging, the animals were immobilized on 5% agarose pads with 0.1 μ m-
216 diameter polystyrene beads (00876-15; Polystyrene suspension). The Bruker
217 Corporations ULTIMA setup was used to perform two-photon imaging and ablations

218 simultaneously (Basu et al., 2017). A 60X water immersion objective was used for
219 ablation and imaging experiments, GFP and mCherry were visualized using 920 nm and
220 1040 nm lasers. A shot for 60 msec pulsed femtosecond IR laser [pulse width 80 fs,
221 irradiation pulse width: 50 msec, laser point spread function (PSF) 400 nm and Z axis
222 PSF-1.5um and wavelength of the laser 720 nm] was used for all ablation experiments.
223 Animals were then examined for successful ablation under a fluorescence microscope.
224 These animals were allowed to grow and recover until they reached the young adult
225 stage. Single animals were then transferred to individual unseeded plates and allowed
226 to habituate for 1 min. Benzaldehyde (concentration of 10^{-1}) was filled in the glass
227 capillary having a small opening pore. The filled capillary was held just in front of the
228 anterior region of the forward moving animals. Videos were recorded for 5 min at 10
229 frames/sec with 5-6 trials leaving a gap of about 1 min between each reading. Graphs
230 were plotted by taking the average value from 5-6 trials, with around 25 animals
231 analyzed for each condition over multiple days. The results were plotted using
232 GraphPad Prism V6 and evaluated using One-Way ANOVA. The mean \pm SEM was
233 plotted.

234 **CRISPR/Cas9 mediated deletion of the *srx-97* gene**

235 The Clustered Regularly Interspaced Short Palindromic Repeats (CRISPR)/Cas9
236 system was used to create the *srx-97* deletion mutation, as described previously
237 (Dickinson and Goldstein, 2016). The two guide RNAs were designed (Hsu et al., 2013)
238 and cloned separately into the *pRB1017* vector under the *CeU6* promoter. The Cas9
239 enzyme was expressed from the *pJW1259* vector under the *erf-3* promoter. The
240 Selection Excision Cassette (SEC) containing plasmid *pDD287* was cloned along-with

241 flanking loxP sites into the *pPD95.75* vector as described previously (Dahiya et al.,
242 2019). The resulting plasmid was used to clone homology arms (500-600 bp) using
243 restriction enzyme based cloning methods.

244 The plasmid mixture containing repair template (40 ng/μl), sgRNA_1 (10 ng/μl),
245 sgRNA_2 (10 ng/μl), *pJW1259* (50 ng/μl), *pCFJ90* (2.5 ng/μl) and *Pvha-6::mCherry* (15
246 ng/μl) was injected into 20-30 adult hermaphrodite animals (containing 4-5 eggs) that
247 were kept at 20 °C. Hygromycin was added after 60 h of injection, directly on the NGM
248 plate containing *C. elegans*. The hygromycin treated plates were left for 10 days at 20
249 °C. Next, 20-30 non-fluorescent rollers were singled out on regular seeded NGM plates.
250 Once 100% roller progeny were observed on the plates, these plates were kept at 34 °C
251 for 3-4 h. Normal moving *C. elegans* were then picked and allowed to produce progeny.
252 The genomic DNA was isolated from these progenies and the desired deletion was
253 confirmed using PCR and sequencing techniques.

254 **Statistical analysis**

255 All statistical analyses on behavioral assays were performed by using GraphPad Prism
256 Version 6.0. The error bars represents SEM. Statistical significance was determined
257 using one-way ANOVA along with the Sadak's *post hoc* test for multiple comparisons.
258 Asterisks in the graphs indicate that the mean differences were statistically significant.
259 The levels of significance were set as “*” $p < 0.05$; “**” $p < 0.01$; “***” $p < 0.001$.

260

261

262

263 **Table 1: Primers used in this study**

Primer number	Forward (FP)/ reverse (RP)	Primer sequence	Gene name	Vector backbone
NK181 NK196	FP RP	atcagcatgcatcttgaaaacctcaatcgaaccag ctctctcccggggacatatcttgaaagttggaat ggag	<i>Psrx-97</i>	<i>pPD49.26_</i> <i>mCherry</i>
NK214 NK196	FP RP	ctctctcgcatgcggaagtttgagcttaggcag ctctctcccggggacatatcttgaaagttggaat ggag	<i>Psrx-97</i>	<i>pPD49.26_</i> <i>mCherry</i>
NK259 NK260	FP RP	ctctctgcatgcggaaccgtattttgtgcaatagtcg ctctctcccggggcaagatgaaattccaaaaag ttattgatatgg	<i>Posm-10</i>	<i>pPD95.75</i>
NK262 NK263	FP RP	ctctctgcatgcgccaaaactgctgaactttg ctctctcccgggcttctgtagaaattcaagactgat cac	<i>Psrb-6</i>	<i>pPD95.75</i>
NK197 NK279	FP RP	ctctctcccgggatgctcttatcgaattggacgc ctctctggtacctcaacatgatcctattcaagttggt attttc	<i>srx-97_</i> <i>UTR</i>	<i>pPD49.26</i>
NK197 NK254	FP RP	ctctctcccgggatgctcttatcgaattggacgc ctctctggtacctcaaaatgtgactgttaaaactgtg actt	<i>srx-97</i> gene	<i>pPD49.26_</i> <i>mCherry</i>
gRNA_ 1		atcaggtctcctctcccactatgactattacagttt tagagctagaaatagcaag	<i>srx-97</i> gene	<i>pRB1017</i>
gRNA_ 2		atcaggtctcctctaaaattataaggcgtaggcag tttagagctagaaatagcaag	<i>srx-97</i> gene	<i>pRB1017</i>
Homolo gy amr_1	FP RP	atcatctagatctccggacgtgaatcttctatc atcagcatgcatcttgaaaacctcaatcgaaccag	<i>srx-97</i> gene	<i>pPD95.75</i>
Homolo gy amr_2	FP RP	atcagggccccattgcacaactgataagatagtcg atcacttaagttcaacatgatcctattcaagttggt	<i>srx-97</i> gene	<i>pPD95.75</i>

NK263	EFP	ctacagtttagtgctgccacag	<i>gpc-1</i>	genotyping
NK264	IFP	tgtcgaaattaaagggtttcgagg		
NK265	RP	gctgtccaacgcaattttcg		
NK303	EFP	gctaggtggagggctgattg	<i>osm-9</i>	genotyping
NK304	IFP	gctaggtggagggctgatta		
NK279	RP	atgggcggtggaagttcg		
NK207	FP	ggatagaagattcacgtccggaag	<i>srx-97</i>	genotyping
NK209	RP	tccatgtggggttgctctg		
NK210	FP	ctccaacatgaaaagcactatcttatcag	<i>srx-97</i>	genotyping
NK179	RP	ttcaacatgatcctattcaagtttgg		
PRS394	FP	gcggttcggatacghaaatactg	<i>tax-4</i>	genotyping
PRS395	ERP	gacggagaagtgtatccgttatatc		
PRS396	IRP	ccatgctcctccctaatcc		
PRS442	FP	cactggcgacgattgtcagatc	<i>tax-2</i>	genotyping
PRS443	ERP	gttattccagtagatgtggccacg		
PRS444	IRP	gtagccaaaatgagttgatctg		
AB37	FP-WT	accttcggctccgactg	<i>glr-1</i>	genotyping
AB38	FP- <i>glr-1</i>	accttcggctccgactta		
AB39	RP	attgaaatgaccataccacc		

264

265

266 FP stands for Forward Primer, RP stands for Reverse Primer, FP-WT stands for

267 External Forward Primer for WT *glr-1* sequence and FP-*glr-1* stands for External268 Forward Primer for *glr-1* sequence in the *glr-1* point mutation line.

269

270

271

272 **Table 2: List of strain used in this study**

Strain name	Genotype	Source
BAB430 (CGC strain CX2205)	<i>odr-3 (n2150)</i>	From CGC (2X outcrossed)
BAB431 (CGC strain CX10)	<i>osm-9 (ky10)</i>	From CGC (3X outcrossed)
BAB432 (CGC strain RB2464)	<i>tax-2 (ok3403)</i>	From CGC (3X outcrossed)
BAB433 (CGC strain VC3113)	<i>tax-4 (ok3771)</i>	From CGC (3X outcrossed)
BAB434 (CGC strain NL792)	<i>gpc-1 (pk298)</i>	From CGC (3X outcrossed)
BAB503 (CGC strain KP4)	<i>glr-1 (n2461)</i>	From CGC (3X outcrossed)
BAB404	<i>srx-97</i>	This study (3X outcrossed)
PY7502	<i>oyls85</i>	From CGC
BAB466	<i>Psrx-97 (600 bp)::mCherry (indEx459)</i>	This study
BAB467	<i>Psrx-97::mCherry (indEx460)</i>	This study
BAB482	<i>srx-97; Psrx-97::SRX-97_ UTR (indEx462)</i>	This study
BAB483	<i>srx-97; Posm-10::SRX-97_ UTR (indEx466)</i>	This study
BAB462	<i>Psrx-97::SRX-97::mCherry (indEx461)</i>	This study
BAB494	<i>srx-97; Psrx-97::SRX-97::mCherry (indEx461)</i>	This study
BAB478	<i>Psrx-97::SRX-97_ UTR (indEx462)</i>	This study
BAB437	<i>Posm-10::SRX-97_ UTR (indEx466)</i>	This study
BAB492	<i>Psrx-97::mCherry (indEx460); Psrb-6::GFP (indEx465)</i>	This study
BAB493	<i>Psrx-97::mCherry (indEx460); Posm-10::GFP</i>	This study

	(<i>indEx464</i>)	
BAB473	<i>srx-97; osm-9</i>	This study
BAB487	<i>srx-97; odr-3</i>	This study
BAB488	<i>srx-97; tax-2</i>	This study
BAB489	<i>srx-97; tax-4</i>	This study
BAB490	<i>srx-97; gpc-1</i>	This study
BAB491	<i>srx-97; oyls85</i>	This study
BAB492	<i>odr-3; oyls85</i>	This study

273

274 **Table 3: Plasmids used in this study**

S. no.	Plasmid ID	Plasmid
1	pBAB459	<i>Psrx-97 (600 bp)::mCherry</i>
2	pBAB460	<i>Psrx-97::mCherry</i>
3	pBAB461	<i>Psrx-97::SRX-97::mCherry</i>
4	pBAB462	<i>Psrx-97::SRX-97_UTR</i>
5	pBAB464	<i>Posm-10::GFP</i>
6	pBAB465	<i>Psrb-6::GFP</i>
7	pBAB466	<i>Posm-10::SRX-97_UTR</i>
8	pBAB472	<i>srx-97_homology arms</i>
9	pBAB470	<i>gRNA_1</i>
10	pBAB471	<i>gRNA_2</i>

275

276 **Table 4: Response of *srx-97* mutants towards multiple water-soluble chemicals**

Water-soluble Chemicals	Genotype	Avoidance in seconds

Glycerol (1 M)	Wild-type (WT)	1.99 ± 0.43 (n=30)
	<i>srx-97</i>	2.42 ± 0.17 (n=33)
	<i>odr-3</i>	3.53 ± 0.25 (n=30) ***
SDS (1%)	WT	1.72 ± 0.23 (n=30)
	<i>srx-97</i>	1.65 ± 0.18 (n=36)
	<i>odr-3</i>	2.86 ± 0.21 (n=32) ***
Cu²⁺ (1 mM)	WT	1.13 ± 0.03 (n=30)
	<i>srx-97</i>	1.10 ± 0.06 (n=30)
	<i>odr-3</i>	1.53 ± 0.25 (n=30) ***
Dihydrocaffeic acid (100 mM)	WT	1.85 ± 0.11 (n=30)
	<i>srx-97</i>	2.52 ± 0.14 (n=30) **
	<i>odr-3</i>	2.36 ± 0.28 (31) **
Dihydrocaffeic acid (1 M)	WT	1.57 ± 0.21 (n=32)
	<i>srx-97</i>	1.68 ± 0.32 (n=31)
	<i>odr-3</i>	1.90 ± 0.15 (n=31)
Acetic acid (0.1 M)	WT	3.88 ± 0.15 (n=31)
	<i>srx-97</i>	3.56 ± 0.10 (n=30)

	<i>odr-3</i>	5.77 ± 0.20 (n=30) ***
Acetic acid (1 M)	WT	2.53 ± 0.15 (n=30)
	<i>srx-97</i>	2.87 ± 0.10 (n=30)
	<i>odr-3</i>	4.58 ± 0.10 (n=30) ***
Quinine (10 mM)	WT	2.49 ± 0.20 (n=35)
	<i>srx-97</i>	2.09 ± 0.21 (n=30)
	<i>odr-3</i>	2.89 ± 0.16 (n=32)
Quinine (1 mM)	WT	10% (n=30)
	<i>srx-97</i>	9% (n=30)
	<i>odr-3</i>	7% (n=30)
M13 Buffer	WT	6% (n=30)
	<i>srx-97</i>	4% (n=30)
	<i>odr-3</i>	4% (n=30)

277

278 **Table 5: Response of *srx-97* mutants towards volatile chemicals**

Volatile chemicals	Genotype	CI index

Diacetyl (10^{-2})	WT	0.81 (n=9)
	<i>srx-97</i>	0.73 (n=9)
	<i>odr-3</i>	0.50** (n=9)
Diacetyl (10^{-3})	WT	0.85 (n=9)
	<i>srx-97</i>	0.84 (n=6)
	<i>odr-3</i>	0.70 (n=6)
Isoamyl alcohol (10^{-2})	WT	0.84 (n=9)
	<i>srx-97</i>	0.83 (n=9)
	<i>odr-3</i>	0.78 (n=9)
Isoamyl alcohol (10^{-3})	WT	0.94 (n=6)
	<i>srx-97</i>	0.92 (n=6)
	<i>odr-3</i>	0.87 (n=6)

279

280 **Results:**

281 **The *P_{srx-97}::mCherry* transgene presents unique expression in the ASH and PHB**
 282 **chemosensory neurons**

283 Chemosensory GPCRs are categorized into nine different classes based on their
 284 sequence homology with the Rhodopsin class of molecules (Fredriksson et al., 2003;
 285 Lagerstrom and Schioth, 2008). The *C. elegans* genome has 1341 genes coding for

286 GPCRs; however, the expression pattern of only 320 genes is known at a single-cell
287 resolution (Robertson and Thomas, 2006; Taniguchi et al., 2014; Vidal et al., 2018).
288 Reports suggest that GPCRs are also expressed in non-neuronal tissues like intestine
289 and are involved in sensing internal cues (Vidal et al., 2018). Some GPCRs change
290 their expression pattern once the animal encounters starvation or dauer-like conditions
291 (Vidal et al., 2018). Despite a large number of studies on the functional and spatial
292 diversity of GPCRs, the expression pattern and function for a majority of the csGPCRs
293 are still unknown (Robertson and Thomas, 2006; Taniguchi et al., 2014; Vidal et al.,
294 2018).

295 We started this study to gain insight into the function of a previously uncharacterized
296 GPCR, SRX-97. SRX-97 was identified in an aldicarb-based RNAi screen and was
297 found to be hypersensitive to aldicarb ((Babu et al., 2011) and Babu et al., unpublished
298 data). To determine the expression pattern of SRX-97, a region 2 kb upstream of the
299 predicted translational start codon of the *srx-97* gene along with six base pairs of the
300 first exonic region were used as a promoter to generate the *Psrx-97::mCherry* reporter
301 line. In these transgenic animals, mCherry expression was specifically detected in a
302 single pair of head amphid neurons and a single pair of tail neurons (Figures 1A, B, D
303 and E). Moreover, even a 600 bp region upstream of the *srx-97* gene with six base pairs
304 from the first exon showed a similar expression pattern as the 2 kb promoter (Figure
305 1C). No expression was detected in any other part of the body. Since the amphid and
306 phasmid neurons are involved in chemotaxis, our data suggested that SRX-97 could
307 specifically be involved in these neurons and likely in chemosensory signaling.

308 Next, we began identifying *Psrx-97::mCherry* expressing neurons based on their cilium
309 morphology, the cell body position in the head and tail region, and colocalization
310 experiments. To uncover the neurons that showed expression of the *srx-97* promoter,
311 we generated the *Psrb-6::GFP* transgenic line, which shows expression in the ASH and
312 ADL neurons in the amphid region (Troemel et al., 1995). The *Psrx-97::mCherry* line
313 presented colocalization in a single neuron pair with the *Psrb-6::GFP* line (Figure 1F,
314 top panel), indicating that *Psrx-97::mCherry* could be expressed in either the ASH or the
315 ADL neurons. To conclusively identify the *Psrx-97::mCherry* expressing neuron, we
316 generated another transgenic line with *Posm-10::GFP*, which shows expression in the
317 amphid ASH and ASI neurons and the PHA/PHB neurons in the phasmid region (Figure
318 1F, bottom panel) and (Hart et al., 1999)). The colocalization of *Psrx-97::mCherry* in a
319 single amphid neuron pair with both marker lines indicated that the *srx-97* promoter
320 drives expression in the ASH neurons. In line with a recent report that suggests that
321 50% of GPCRs which express in ASH neurons also show expression in the PHB neuron
322 (Vidal et al., 2018), we found that in the tail region, *Psrx-97::mCherry* showed
323 colocalization with a pair of phasmid neurons (Figure 1G, top panels indicating
324 colocalization with one phasmid neuron). Based on the orientation of the animal
325 (posterior right and ventral down), this neuron appears to be the PHB neuron (Figure
326 1G, DIC image in bottom panel).

327 We then analyzed a SRX-97 translational reporter and found that the *Psrx-97::SRX-*
328 *97::mCherry* transgenic line showed SRX-97 protein localization towards the cilium tip
329 of the ASH neurons (Figure 1H), indicating that this protein may be involved in sensing
330 environmental cues from the surroundings.

331 **CRISPR/Cas9 mediated deletion of *srx-97***

332 *C. elegans* have 13 pairs of chemosensory neurons in the anterior amphid and posterior
333 phasmid regions. However, it can detect several different chemical cues ranging from
334 volatile to water-soluble odorants through diverse GPCRs (Robertson and Thomas,
335 2006; Vidal et al., 2018). Seven percent of the *C. elegans* genome encodes for
336 chemoreceptors. However, only around 900 chemoreceptor genes have been
337 characterized functionally, many through RNAi experiments (Robertson and Thomas,
338 2006; Taniguchi et al., 2014; Vidal et al., 2018). Hence, only a few mutant lines of
339 GPCRs are available. Our studies have shown that the *srx-97* promoter drives
340 expression in ASH and PHB neurons. This expression pattern raised the possibility that
341 it might function as a receptor for odorant/s. Since no mutant strain was available for
342 this gene, we utilized the CRISPR/Cas9 based strategy to generate a deletion in the
343 *srx-97* gene.

344 The SRX-97 GPCR is part of the SRX family of proteins that belong to the SRG
345 superfamily that encodes around 320 genes (Robertson and Thomas, 2006; Vidal et al.,
346 2018). The *srx-97* gene encodes a predicted protein of 317 amino acids (Figure 2A).
347 Hydrophobicity analyses showed that the SRX-97 protein encodes for a seven-
348 transmembrane domain protein, with the characteristic topology of GPCRs (Figure 2A).
349 By utilizing the gene-editing CRISPR/Cas9 technique, we made a complete deletion of
350 the *srx-97* gene (from 61 bp of the first exon to the 3' UTR region, deleting a 1834 bp
351 sequence) (Figures 2B and C). We next performed aldicarb assays with the *srx-97*
352 deletion animals and found no significant difference in aldicarb sensitivity between the
353 deletion strain and wild-type (WT) control animals (Figure 2-1A). This data, along with

354 the localization and expression pattern of SRX-97, indicated that SRX-97 likely did not
355 function at the neuromuscular junction to cause defects in aldicarb sensitivity. The
356 aldicarb phenotype in the RNAi screen could have been a false positive due to cross-
357 complementation reactions with other GPCRs. Hence, we proceeded to study the role
358 of SRX-97 in other processes.

359 **Loss of *srx-97* leads to defects in chemotaxis towards benzaldehyde**

360 ASH is a polymodal neuron that can respond to noxious, mechanical and osmotic
361 stimuli (Colbert et al., 1997; Hilliard et al., 2005; Hilliard et al., 2004; Kaplan and Horvitz,
362 1993). To characterize the role of the SRX-97 GPCR in ASH neurons, we examined the
363 response of the *srx-97* mutant line towards several compounds including glycerol, SDS,
364 Cu^{2+} , quinine, dihydrocaffeic acid and acetic acid (Hilliard et al., 2005; Hilliard et al.,
365 2002; Kaplan and Horvitz, 1993). The *srx-97* mutant animals showed minor defects in
366 avoidance behavior towards 2 M glycerol and 100 mM dihydrocaffeic acid (DHCA) when
367 compared to the control wild-type (WT) animals (Figure 3A and Table 4). We also tested
368 the behavior of *srx-97* mutants to other chemicals and found that *srx-97* did not show
369 significant differences when compared to WT control animals in their behavior towards
370 glycerol (1 M), SDS (0.1% and 1%), Cu^{2+} (1 mM and 10 mM), quinine (1 mM and 10
371 mM), dihydrocaffeic acid (1 M) and acetic acid (1 M and 0.1 M) (Figure 3 B, C and Table
372 4). Mutants in *odr-3*, a $\text{G}\alpha$ protein, were used as controls for these avoidance assays,
373 since *odr-3* has been reported to be involved in multiple behaviors controlled by the
374 ASH neurons (Hilliard et al., 2005; Hilliard et al., 2004; Roayaie et al., 1998; Zhang et
375 al., 2016). The ASH neurons are also known to play a role in sensing mechanical stimuli
376 (Kaplan and Horvitz, 1993). In order to test the role of SRX-97 in mechanosensation, we

377 performed a nose touch assay with WT, *srx-97*, and *glr-1* (defective for nose touch
378 assay) (Maricq et al., 1995) animals. Upon performing the assays, we observed that
379 *srx-97* mutant animals did not show significant defects in nose touch assays when
380 compared with WT controls (Figure 3D). These data indicates that loss of *srx-97* does
381 not affect many aspects of the general ASH neuronal responses.

382 The ASH neurons are also known to be involved in detecting volatile chemicals
383 (Troemel et al., 1995). To analyze the role of SRX-97 in detecting volatile chemicals, we
384 used a modified chemotaxis plate, having four quadrants, two opposite quadrants for
385 test solutions (T), and two for control solutions (C) (illustrated in Figure 3-1A). Both
386 control and test spots were 3 cm away from the *C. elegans* loading center. Before the
387 addition of control or test solution, we added sodium azide to paralyze the animals once
388 they reach their respective spots. Next, we calculated the chemotaxis index by
389 measuring the number of animals in each quadrant with the formula shown in Figure 3-
390 1A. Previous work has shown that in chemotaxis assays, the ASH neurons are involved
391 in aversive behaviors towards the repellent 1-octanol (Chao et al., 2004). Here again,
392 we found no significant change in the chemotaxis index of the *srx-97* mutant line when
393 compared to WT control animals (Figure 3E). Recent findings suggest that the ASH
394 neurons are involved in sensing high concentrations of chemicals, such as isoamyl
395 alcohol (IAA) (Yoshida et al., 2012) and diacetyl (DA) (Taniguchi et al., 2014). In the
396 chemotaxis assays, we used a range of concentrations of IAA and DA, testing for any
397 defects in responses towards these chemicals. We found that the *srx-97* mutants did
398 not show any significant defects in chemotaxis towards IAA and DA when compared to
399 control animals (Figure 3F and Table 5).

400 The ASH neurons are also known to be involved in detecting benzaldehyde (Aoki et al.,
401 2011; Taniguchi et al., 2014; Troemel et al., 1995; Walker et al., 2009). A previously
402 identified GPCR, DCAR-1, has homology with the SRX family of proteins and *dcar-1*
403 mutants show defective chemotaxis towards undiluted benzaldehyde (Aoki et al., 2011).
404 In our chemotaxis assays we found that the *srx-97* mutant animals showed significantly
405 more attraction to a high concentration of benzaldehyde (10^{-1}) when compared to WT
406 controls animals (Figure 3G). We also found that as reported previously *odr-3* mutant
407 animals showed reduced attraction towards benzaldehyde (Figure 3G and (Roayaie et
408 al., 1998)). At low concentrations (10^{-2} and 10^{-3}) of benzaldehyde and undiluted
409 benzaldehyde, there was no significant difference between *srx-97* and WT animals
410 (Figure 3G). Earlier reports indicate that the ASH neurons are involved in responding to
411 high concentrations of benzaldehyde (0.1% v/v), whereas medium or low concentrations
412 (0.005-0.0001%) of benzaldehyde are sensed by the AWC and AWA neurons
413 (Leinwand et al., 2015). Since SRX-97 is expressed in the ASH neurons, it could be
414 involved in sensing a very high concentration range of benzaldehyde. In order to
415 confirm the *srx-97* mutant phenotype, we tried to rescue the defects seen in the *srx-97*
416 mutants. We found that the defects in chemotaxis towards benzaldehyde seen in the
417 *srx-97* animals could be rescued by expressing SRX-97 under its endogenous
418 promoter, and partially rescued by expressing SRX-97 under the *osm-10* promoter that
419 drives expression in the ASH and ASI neurons (Figure 3H). Although we observed
420 rescue of the *srx-97* mutants with the *srx-97* and the *osm-10* promoter lines, we also
421 found a small but significant rescue in animals that did not carry any observable
422 rescuing arrays, possibly due to low expression of the rescuing array that was

423 undetectable with the fluorescence markers in these non-array (NA) lines. Further, in
424 the WT background, the rescuing lines of SRX-97 behaved in a manner similar to WT
425 control animals (Figure 3-1B). We also tested the previously described mCherry-tagged
426 SRX-97 line (Figure 1H) in our rescue experiments and observed a partial rescue of the
427 *srx-97* mutant phenotype (Figure 3-1C, the rescue line showed no significant difference
428 with respect to WT control animals or *srx-97* mutants). This partial rescue could be by
429 the mCherry tag hindering the function of SRX-97 or due to incomplete penetrance of
430 expression from the arrays used. Thus far our data suggest that the csGPCR SRX-97 is
431 responsible for sensing high concentrations of benzaldehyde.

432 **Ablation of ASH causes defects in benzaldehyde sensing**

433 We next analyzed the chemotaxis frequency of *srx-97* mutants towards high
434 concentrations of benzaldehyde (Nuttley et al., 2001). Here we added the benzaldehyde
435 (10^{-1}) on a small sheet (0.5-1 cm diameter) of parafilm so it would not be soaked in the
436 media. We also excluded the addition of sodium azide on the control and test spots so
437 as to allow the animals to move freely towards the control or test spots (Illustrated in
438 Figure 4A). After a 60 min incubation period, the animals were counted along each
439 sector, and the chemotaxis frequency was calculated by the formula indicated in Figure
440 4A. Again, the *srx-97* mutants showed a significant increase in their attraction towards
441 benzaldehyde (Figure 4B). This defect was reduced by expressing SRX-97 under its
442 endogenous promoter, suggesting that SRX-97 is responsible for sensing high
443 concentrations of benzaldehyde and that the *srx-97* phenotype may not be due to the
444 initial attraction followed by repulsion behavior shown by the *odr-3* mutants (Figure 4B
445 and (Nuttley et al., 2001)). However, a similar reduction of the defect was also observed

446 in non-transgenic siblings that could be due to low expression of the rescuing array
447 undetectable by fluorescence (Figure 4B).

448 In order to further strengthen our data that SRX-97 was indeed acting in ASH to sense
449 high concentrations of benzaldehyde, we ablated the ASH neurons in WT as well as in
450 *srx-97* mutant animals. We then tested the delay in response towards benzaldehyde in
451 mock ablated and ASH ablated animals. Our data shows that WT animals with ablated
452 ASH neurons show a significant delay in their response to benzaldehyde when
453 compared to the mock-ablated animals (Figure 4C). Moreover, there was a significant
454 difference in ASH ablated WT animals and mock ablated *srx-97* mutant *C. elegans*,
455 indicating that ASH may also have other receptors that allows detection of high
456 concentrations of benzaldehyde. Animals where the ASH neurons were ablated in *srx-*
457 *97* mutants, behaved like WT animals that had undergone ASH neuron ablation, further
458 indicating the function of SRX-97 in ASH neurons.

459 **Defects in sensory signaling appear to function downstream of *srx-97***

460 The ASH neurons express multiple GPCR associated sensory molecules that are
461 reported to be required for signal transduction (Hilliard et al., 2005; Hilliard et al., 2004;
462 Roayaie et al., 1998). Among these, the G protein subunit, GPC-1 that encodes the γ
463 subunit of GPCRs, shows a positive adaptive olfactory response towards benzaldehyde
464 (Jansen et al., 2002; Yamada et al., 2009). We found that *gpc-1* and *srx-97* double
465 mutants show a negative chemotaxis index similar to what was seen with *gpc-1* mutant
466 animals (Figure 5A). These data indicated that SRX-97 could be functioning through the
467 G-protein signaling pathway. We next tested mutants in ODR-3, a $G\alpha$ protein which is
468 primarily required for sensory signal transduction and is involved in responses towards

469 osmotic strength, high salt concentration, nose touch and volatile chemicals (Hilliard et
470 al., 2005; Hilliard et al., 2004; Roayaie et al., 1998; Zhang et al., 2016). Mutants in *odr-3*
471 have been reported to show defects in attraction towards low concentrations of
472 benzaldehyde (1:200) (Roayaie et al., 1998). In our assay, we found that *odr-3* and *srx-*
473 *97*; *odr-3* double mutants showed negative chemotaxis indices towards high
474 concentration of benzaldehyde, similar to what was seen with *gpc-1* mutants (Figure
475 5B). These data further suggest that SRX-97 could be involved in chemotactic function
476 through the GPCR pathway.

477 The AWC neurons sense low concentration of benzaldehyde through *odr-3* signaling
478 (Bargmann et al., 1993). To gain more insight into the function of AWC neurons in
479 sensing benzaldehyde, we used a line where AWC is ablated (AWC(-) (Beverly et al.,
480 2011). We found that the loss of AWC neurons made the *C. elegans* aversive towards
481 benzaldehyde (Figure 5B). Further loss of *srx-97* in the AWC (-) background did not
482 appear to affect the AWC(-) phenotype (Figure 5B). These data suggest that AWC is
483 the primary sensory neuron that shows attraction to diffused (in our assay) or low
484 concentrations of benzaldehyde. Further, the ASH neurons could act as secondary sets
485 of neurons that are responsive to high benzaldehyde concentrations as shown
486 previously for IAA (Yoshida et al., 2012). We also found that the loss of *odr-3* in the
487 AWC (-) animals appeared to significantly suppress the AWC ablation defects with
488 respect to chemotaxis towards benzaldehyde (Figure 5B). Studies have shown that
489 ODR-3 is expressed in ASH, AWA, AWB and AWC neurons (Roayaie et al., 1998).
490 Hence it is possible that ODR-3 might be affecting chemotaxis towards benzaldehyde
491 through neurons other than AWC.

492 We next analyzed the molecules that may be functioning downstream of the SRX-97
493 GPCR. The ASH neurons express multiple channel proteins that get activated through
494 GPCRs and are involved in regulating different behavioral outputs (Sengupta, 2007).
495 One such molecule, OSM-9, is a member of the vanilloid subfamily of Transient
496 Receptor Potential (TRP) channel proteins that regulates avoidance behaviors to
497 osmotic strength, nose touch and undiluted benzaldehyde in the ASH neurons (Colbert
498 et al., 1997; Murayama and Maruyama, 2013; Zou et al., 2017). We found that *osm-9*
499 mutants showed a phenotype similar to that seen in WT animals when tested for a high
500 concentration of benzaldehyde (Figure 5A). The cyclic nucleotide-gated channel
501 proteins, TAX-2 and TAX-4 are responsible for the detection of volatile chemicals like
502 benzaldehyde by AWC and other amphid neurons, although the source of activating
503 cGMP is still unknown (Coburn and Bargmann, 1996; Komatsu et al., 1996; Zagotta and
504 Siegelbaum, 1996). These mutants were tested for defects in chemotaxis to
505 benzaldehyde and showed a negative chemotaxis index toward a high concentration of
506 benzaldehyde (Figure 5A). All three mutants, *osm-9*, *tax-2*, and *tax-4*, completely
507 suppressed the increased chemotaxis behavior seen in *srx-97* mutant animals. The
508 suppression of the *srx-97* mutant phenotype by these downstream molecules indicates
509 that either the SRX-97 GPCR acts redundantly to sense the high concentrations of
510 benzaldehyde by activating pathways different from the ones tested, or OSM-9, TAX-2
511 and TAX-4 function to detect both high and low concentrations of benzaldehyde and
512 SRX-97 functions through the canonical G-protein pathway to elicit responses to high
513 concentrations of benzaldehyde.

514

515 **Discussion**

516 In this study, we have characterized the expression and function of the GPCR, SRX-97.
517 From our expression studies, it is clear that SRX-97 shows expression in the ASH and
518 PHB neurons. Moreover, the chemotaxis experiments reveal that the GPCR SRX-97
519 senses high concentrations of benzaldehyde. Our data indicate that in comparison with
520 wild-type (WT) animals, *srx-97* null mutant animals show increased attraction towards
521 high concentrations of benzaldehyde (10^{-1}). We also show that SRX-97::mCherry driven
522 by its native promoter shows localization along the ciliary tip of the ASH neurons. Since
523 the cilia are the compartment where signal sensation and transduction occurs, the
524 localization of SRX-97 at the cilium tips suggests its role in sensory perception or
525 transduction of sensory signal/s. These results suggest that SRX-97 expressed in the
526 ASH neurons is responsible for detecting benzaldehyde from its surroundings.

527 Other than SRX-97, ASH neurons also express different sets of GPCRs, which sense
528 benzaldehyde (Aoki et al., 2011; Taniguchi et al., 2014; Vidal et al., 2018). For example,
529 DCAR-1 is expressed in ASH neurons and is involved in sensing undiluted
530 benzaldehyde (Aoki et al., 2011). Multiple reports propose that there is a “tuning curve”
531 for the olfactory neurons through which some olfactory receptors exhibit noticeable
532 sensitivity (threshold) for some odorants; some neurons are activated by receptors only
533 at low odorant concentrations, while other neurons and receptors are activated at high
534 concentrations of odorants (Firestein, 2001; Spehr and Munger, 2009). Since the *srx-*
535 *97* mutant animals show reduced but not completely abolished response towards high
536 concentrations (10^{-1}) of benzaldehyde (Figure 3G and Figure 4C), it is possible that
537 SRX-97 acts as a constituent of a receptor complex on the ASH neurons allowing for

538 detection of benzaldehyde at high or undiluted concentrations but not at low
539 concentrations. On the contrary, low concentrations of benzaldehyde are sensed by
540 the AWC neurons (Bargmann et al., 1993; Leinwand et al., 2015). The wild-type like
541 chemotaxis response of *srx-97* mutants towards undiluted and low concentration of
542 benzaldehyde may suggest that animals sense their surrounding by activating different
543 receptors using the corresponding neurons in a concentration-dependent manner and
544 this, in turn, leads to appropriate behavioral responses.

545 GPCRs signal through heteromeric G-proteins signaling cascades and transduce
546 signals from the environment through intracellular mediators that play a vital role in
547 triggering behavior. The ASH and other amphid neurons express the G α protein ODR-3
548 as well as OSM-9, a TRPV protein that is involved in the sensation of various stimuli
549 including olfaction (Bargmann et al., 1993; Hilliard et al., 2004; Roayaie et al., 1998;
550 Troemel et al., 1997). The amphid AWC neurons act as primary olfactory neurons
551 involved in sensing low concentrations of benzaldehyde (Leinwand et al., 2015), while
552 the ASH neurons are required for sensing undiluted benzaldehyde (Colbert et al., 1997;
553 Tobin et al., 2002; Troemel et al., 1995). In our chemotaxis assay (90 minutes), we
554 found that *srx-97* mutants presented chemotaxis defects towards high concentrations of
555 benzaldehyde; in these assays the animals were placed 3 cm away from the source of
556 benzaldehyde and hence not at short range from the source (Troemel et al., 1995).
557 Previous work has shown that the distance or diffusion gradient of a test chemical may
558 activate primary sensory neurons like AWA and AWC (Leinwand et al., 2015; Taniguchi
559 et al., 2014; Yoshida et al., 2012). Our work also indicates that defects in the

560 downstream signaling molecules in these neurons could affect the repulsion of the
561 animals from the source.

562 The defects seen in the *srx-97* mutation towards dihydrocaffeic acid (DHCA) is similar to
563 the previously reported GPCR/*dcar-1* mutants expressed in ASH neurons (Aoki et al.,
564 2011). DCAR-1 functions through *odr-3* and *osm-9* signaling pathways to elicit its
565 response towards DHCA (Aoki et al., 2011). However, the downstream molecules for
566 the signaling pathway remain unidentified. We also see that *srx-97* mutant animals
567 show defects towards high osmolarity as seen in experiments using 2 M glycerol.
568 Although in our battery of tests we saw small but significant defects in *srx-97* mutants
569 towards 2 M glycerol and 100 mM dihydrocaffeic acid, we do not know the mechanisms
570 underlying these defects in the mutant animals. It will be interesting in future to
571 understand how single GPCRs like SRX-97 and their associated proteins or
572 downstream molecules are responsible for these different aspects of chemosensation in
573 *C. elegans*.

574 Our results propose that there could be alternative pathways for signal transduction in
575 ASH neurons through GPCRs like SRX-97. To our knowledge, downstream signaling
576 molecules, the loss of which causes attraction to an undiluted or high concentration of
577 benzaldehyde through the ASH neurons have not yet been identified. The *C.*
578 *elegans* genome encodes for 21 G α , 2 G β and 2 G γ genes (Cuppen et al., 2003;
579 Jansen et al., 1999). Out of these, 11 G α proteins are expressed in the ASH neurons
580 (Bastiani and Mendel, 2006). Our results suggest that the ASH neurons are involved in
581 aversion to undiluted or high concentrations of benzaldehyde through multiple or

582 redundant chemosensory pathways involved in the signaling through GPCRs like SRX-
583 97.

584 In conclusion, our results bring out the possibility that SRX-97 is a key mediator in
585 chemotaxis towards high concentrations of benzaldehyde in the chemosensory system
586 of *C. elegans*. However, the downstream signaling components still need to be
587 identified, in order to provide more details into the functioning of SRX-97 in the ASH
588 neurons. These investigations may offer insights into the nature of signal transduction in
589 ASH neurons and their physiological role in concentration dependent avoidance
590 responses.

591

592

593

594

595

596

597

598

599

600

601

602

603

604 **References**

- 605 Aoki, R., Yagami, T., Sasakura, H., Ogura, K., Kajihara, Y., Ibi, M., Miyamae, T.,
606 Nakamura, F., Asakura, T., Kanai, Y., *et al.* (2011). A seven-transmembrane receptor
607 that mediates avoidance response to dihydrocaffeic acid, a water-soluble repellent in
608 *Caenorhabditis elegans*. *The Journal of neuroscience : the official journal of the Society*
609 *for Neuroscience* *31*, 16603-16610.
- 610 Avery, L., and Horvitz, H.R. (1987). A cell that dies during wild-type *C. elegans*
611 development can function as a neuron in a *ced-3* mutant. *Cell* *51*, 1071-1078.
- 612 Avery, L., and Horvitz, H.R. (1989). Pharyngeal pumping continues after laser killing of
613 the pharyngeal nervous system of *C. elegans*. *Neuron* *3*, 473-485.
- 614 Babu, K., Hu, Z., Chien, S.C., Garriga, G., and Kaplan, J.M. (2011). The
615 immunoglobulin super family protein RIG-3 prevents synaptic potentiation and regulates
616 Wnt signaling. *Neuron* *71*, 103-116.
- 617 Bargmann, C.I. (2006). Chemosensation in *C. elegans*. *WormBook*, 1-29.
- 618 Bargmann, C.I., Hartwig, E., and Horvitz, H.R. (1993). Odorant-selective genes and
619 neurons mediate olfaction in *C. elegans*. *Cell* *74*, 515-527.
- 620 Bargmann, C.I., and Horvitz, H.R. (1991). Chemosensory neurons with overlapping
621 functions direct chemotaxis to multiple chemicals in *C. elegans*. *Neuron* *7*, 729-742.
- 622 Bastiani, C., and Mendel, J. (2006). Heterotrimeric G proteins in *C. elegans*.
623 *WormBook*, 1-25.
- 624 Basu, A., Dey, S., Puri, D., Das Saha, N., Sabharwal, V., Thyagarajan, P., Srivastava,
625 P., Koushika, S.P., and Ghosh-Roy, A. (2017). *let-7* miRNA controls CED-7 homotypic
626 adhesion and EFF-1-mediated axonal self-fusion to restore touch sensation following
627 injury. *Proceedings of the National Academy of Sciences of the United States of*
628 *America* *114*, E10206-E10215.
- 629 Beverly, M., Anbil, S., and Sengupta, P. (2011). Degeneracy and neuromodulation
630 among thermosensory neurons contribute to robust thermosensory behaviors in
631 *Caenorhabditis elegans*. *The Journal of neuroscience : the official journal of the Society*
632 *for Neuroscience* *31*, 11718-11727.
- 633 Bhardwaj, A., Pandey, P., and Babu, K. (2020). Control of Locomotory Behavior of
634 *Caenorhabditis elegans* by the Immunoglobulin Superfamily Protein RIG-3. *Genetics*
635 *214*, 135- 145.
- 636 Bhardwaj, A., Thapliyal, S., Dahiya, Y., and Babu, K. (2018). FLP-18 Functions through
637 the G-Protein-Coupled Receptors NPR-1 and NPR-4 to Modulate Reversal Length in
638 *Caenorhabditis elegans*. *The Journal of neuroscience : the official journal of the Society*
639 *for Neuroscience* *38*, 4641-4654.
- 640 Brenner, S. (1974). The genetics of *Caenorhabditis elegans*. *Genetics* *77*, 71-94.
- 641 Chao, M.Y., Komatsu, H., Fukuto, H.S., Dionne, H.M., and Hart, A.C. (2004). Feeding
642 status and serotonin rapidly and reversibly modulate a *Caenorhabditis elegans*
643 chemosensory circuit. *Proceedings of the National Academy of Sciences of the United*
644 *States of America* *101*, 15512-15517.
- 645 Coburn, C.M., and Bargmann, C.I. (1996). A putative cyclic nucleotide-gated channel is
646 required for sensory development and function in *C. elegans*. *Neuron* *17*, 695-706.
- 647 Colbert, H.A., Smith, T.L., and Bargmann, C.I. (1997). OSM-9, a novel protein with
648 structural similarity to channels, is required for olfaction, mechanosensation, and

- 649 olfactory adaptation in *Caenorhabditis elegans*. The Journal of neuroscience : the
650 official journal of the Society for Neuroscience 17, 8259-8269.
- 651 Cuppen, E., van der Linden, A.M., Jansen, G., and Plasterk, R.H. (2003). Proteins
652 interacting with *Caenorhabditis elegans* Galpha subunits. Comp Funct Genomics 4,
653 479-491.
- 654 Dahiya, Y., Rose, S., Thapliyal, S., Bhardwaj, S., Prasad, M., and Babu, K. (2019).
655 Differential Regulation of Innate and Learned Behavior by Creb1/CRH-1 in
656 *Caenorhabditis elegans*. The Journal of neuroscience : the official journal of the Society
657 for Neuroscience 39, 7934-7946.
- 658 Dickinson, D.J., and Goldstein, B. (2016). CRISPR-Based Methods for *Caenorhabditis*
659 *elegans* Genome Engineering. Genetics 202, 885-901.
- 660 Erlandson, S.C., McMahon, C., and Kruse, A.C. (2018). Structural Basis for G Protein-
661 Coupled Receptor Signaling. Annu Rev Biophys.
- 662 Firestein, S. (2001). How the olfactory system makes sense of scents. Nature 413, 211-
663 218.
- 664 Fredriksson, R., Lagerstrom, M.C., Lundin, L.G., and Schiöth, H.B. (2003). The G-
665 protein-coupled receptors in the human genome form five main families. Phylogenetic
666 analysis, paralogon groups, and fingerprints. Mol Pharmacol 63, 1256-1272.
- 667 Gray, J.M., Hill, J.J., and Bargmann, C.I. (2005). A circuit for navigation in
668 *Caenorhabditis elegans*. Proceedings of the National Academy of Sciences of the
669 United States of America 102, 3184-3191.
- 670 Hart, A.C., Kass, J., Shapiro, J.E., and Kaplan, J.M. (1999). Distinct signaling pathways
671 mediate touch and osmosensory responses in a polymodal sensory neuron. The
672 Journal of neuroscience : the official journal of the Society for Neuroscience 19, 1952-
673 1958.
- 674 Hilliard, M.A., Apicella, A.J., Kerr, R., Suzuki, H., Bazzicalupo, P., and Schafer, W.R.
675 (2005). In vivo imaging of *C. elegans* ASH neurons: cellular response and adaptation to
676 chemical repellents. The EMBO journal 24, 63-72.
- 677 Hilliard, M.A., Bargmann, C.I., and Bazzicalupo, P. (2002). *C. elegans* responds to
678 chemical repellents by integrating sensory inputs from the head and the tail. Current
679 biology : CB 12, 730-734.
- 680 Hilliard, M.A., Bergamasco, C., Arbucci, S., Plasterk, R.H., and Bazzicalupo, P. (2004).
681 Worms taste bitter: ASH neurons, QUI-1, GPA-3 and ODR-3 mediate quinine avoidance
682 in *Caenorhabditis elegans*. The EMBO journal 23, 1101-1111.
- 683 Hsu, P.D., Scott, D.A., Weinstein, J.A., Ran, F.A., Konermann, S., Agarwala, V., Li, Y.,
684 Fine, E.J., Wu, X., Shalem, O., *et al.* (2013). DNA targeting specificity of RNA-guided
685 Cas9 nucleases. Nat Biotechnol 31, 827-832.
- 686 Jansen, G., Thijssen, K.L., Werner, P., van der Horst, M., Hazendonk, E., and Plasterk,
687 R.H. (1999). The complete family of genes encoding G proteins of *Caenorhabditis*
688 *elegans*. Nature genetics 21, 414-419.
- 689 Jansen, G., Weinkove, D., and Plasterk, R.H. (2002). The G-protein gamma subunit
690 gpc-1 of the nematode *C.elegans* is involved in taste adaptation. The EMBO journal 21,
691 986-994.
- 692 Kaplan, J.M., and Horvitz, H.R. (1993). A dual mechanosensory and chemosensory
693 neuron in *Caenorhabditis elegans*. Proceedings of the National Academy of Sciences of
694 the United States of America 90, 2227-2231.

- 695 Katritch, V., Cherezov, V., and Stevens, R.C. (2013). Structure-function of the G
696 protein-coupled receptor superfamily. *Annu Rev Pharmacol Toxicol* 53, 531-556.
- 697 Komatsu, H., Mori, I., Rhee, J.S., Akaike, N., and Ohshima, Y. (1996). Mutations in a
698 cyclic nucleotide-gated channel lead to abnormal thermosensation and chemosensation
699 in *C. elegans*. *Neuron* 17, 707-718.
- 700 Lagerstrom, M.C., and Schiöth, H.B. (2008). Structural diversity of G protein-coupled
701 receptors and significance for drug discovery. *Nat Rev Drug Discov* 7, 339-357.
- 702 Leinwand, S.G., Yang, C.J., Bazopoulou, D., Chronis, N., Srinivasan, J., and Chalasani,
703 S.H. (2015). Circuit mechanisms encoding odors and driving aging-associated
704 behavioral declines in *Caenorhabditis elegans*. *Elife* 4, e10181.
- 705 Mahoney, T.R., Luo, S., and Nonet, M.L. (2006). Analysis of synaptic transmission in
706 *Caenorhabditis elegans* using an aldicarb-sensitivity assay. *Nat Protoc* 1, 1772-1777.
- 707 Margie, O., Palmer, C., and Chin-Sang, I. (2013). *C. elegans* chemotaxis assay. *J Vis*
708 *Exp*, e50069.
- 709 Maricq, A.V., Peckol, E., Driscoll, M., and Bargmann, C.I. (1995). Mechanosensory
710 signalling in *C. elegans* mediated by the GLR-1 glutamate receptor. *Nature* 378, 78-81.
- 711 Mello, C., and Fire, A. (1995). DNA transformation. *Methods in cell biology* 48, 451-482.
- 712 Mello, C.C., Kramer, J.M., Stinchcomb, D., and Ambros, V. (1991). Efficient gene
713 transfer in *C.elegans*: extrachromosomal maintenance and integration of transforming
714 sequences. *The EMBO journal* 10, 3959-3970.
- 715 Murayama, T., and Maruyama, I.N. (2013). Decision making in *C. elegans* chemotaxis
716 to alkaline pH: Competition between two sensory neurons, ASEL and ASH.
717 *Communicative & integrative biology* 6, e26633.
- 718 Nuttley, W.M., Harbinder, S., and van der Kooy, D. (2001). Regulation of distinct
719 attractive and aversive mechanisms mediating benzaldehyde chemotaxis in
720 *Caenorhabditis elegans*. *Learning & memory* 8, 170-181.
- 721 Pokala, N., Liu, Q., Gordus, A., and Bargmann, C.I. (2014). Inducible and titratable
722 silencing of *Caenorhabditis elegans* neurons in vivo with histamine-gated chloride
723 channels. *Proceedings of the National Academy of Sciences of the United States of*
724 *America* 111, 2770-2775.
- 725 Roayaie, K., Crump, J.G., Sagasti, A., and Bargmann, C.I. (1998). The G alpha protein
726 ODR-3 mediates olfactory and nociceptive function and controls cilium morphogenesis
727 in *C. elegans* olfactory neurons. *Neuron* 20, 55-67.
- 728 Robertson, H.M., and Thomas, J.H. (2006). The putative chemoreceptor families of *C.*
729 *elegans*. *WormBook*, 1-12.
- 730 Russell, J.S.a.D. (2001). *Molecular Cloning: A Laboratory Manual*.
- 731 Sengupta, P. (2007). Generation and modulation of chemosensory behaviors in *C.*
732 *elegans*. *Pflugers Arch* 454, 721-734.
- 733 Sengupta, P., Chou, J.H., and Bargmann, C.I. (1996). *odr-10* encodes a seven
734 transmembrane domain olfactory receptor required for responses to the odorant
735 diacetyl. *Cell* 84, 899-909.
- 736 Spehr, M., and Munger, S.D. (2009). Olfactory receptors: G protein-coupled receptors
737 and beyond. *J Neurochem* 109, 1570-1583.
- 738 Taniguchi, G., Uozumi, T., Kiriya, K., Kamizaki, T., and Hirotsu, T. (2014). Screening
739 of odor-receptor pairs in *Caenorhabditis elegans* reveals different receptors for high and
740 low odor concentrations. *Sci Signal* 7, ra39.

- 741 Tobin, D.M., Madsen, D.M., Kahn-Kirby, A., Peckol, E.L., Moulder, G., Barstead, R.,
742 Maricq, A.V., and Bargmann, C.I. (2002). Combinatorial expression of TRPV channel
743 proteins defines their sensory functions and subcellular localization in *C. elegans*
744 neurons. *Neuron* **35**, 307-318.
- 745 Troemel, E.R., Chou, J.H., Dwyer, N.D., Colbert, H.A., and Bargmann, C.I. (1995).
746 Divergent seven transmembrane receptors are candidate chemosensory receptors in *C.*
747 *elegans*. *Cell* **83**, 207-218.
- 748 Troemel, E.R., Kimmel, B.E., and Bargmann, C.I. (1997). Reprogramming chemotaxis
749 responses: sensory neurons define olfactory preferences in *C. elegans*. *Cell* **91**, 161-
750 169.
- 751 Vidal, B., Aghayeva, U., Sun, H., Wang, C., Glenwinkel, L., Bayer, E.A., and Hobert, O.
752 (2018). An atlas of *Caenorhabditis elegans* chemoreceptor expression. *PLoS biology*
753 **16**, e2004218.
- 754 Walker, D.S., Vazquez-Manrique, R.P., Gower, N.J., Gregory, E., Schafer, W.R., and
755 Baylis, H.A. (2009). Inositol 1,4,5-trisphosphate signalling regulates the avoidance
756 response to nose touch in *Caenorhabditis elegans*. *PLoS genetics* **5**, e1000636.
- 757 Yamada, K., Hirotsu, T., Matsuki, M., Kunitomo, H., and Iino, Y. (2009). GPC-1, a G
758 protein gamma-subunit, regulates olfactory adaptation in *Caenorhabditis elegans*.
759 *Genetics* **181**, 1347-1357.
- 760 Yoshida, K., Hirotsu, T., Tagawa, T., Oda, S., Wakabayashi, T., Iino, Y., and Ishihara, T.
761 (2012). Odour concentration-dependent olfactory preference change in *C. elegans*. *Nat*
762 *Commun* **3**, 739.
- 763 Zagotta, W.N., and Siegelbaum, S.A. (1996). Structure and function of cyclic nucleotide-
764 gated channels. *Annu Rev Neurosci* **19**, 235-263.
- 765 Zhang, C., Zhao, N., Chen, Y., Zhang, D., Yan, J., Zou, W., Zhang, K., and Huang, X.
766 (2016). The Signaling Pathway of *Caenorhabditis elegans* Mediates Chemotaxis
767 Response to the Attractant 2-Heptanone in a Trojan Horse-like Pathogenesis. *The*
768 *Journal of biological chemistry* **291**, 23618-23627.
- 769 Zheng, M., Cao, P., Yang, J., Xu, X.Z., and Feng, Z. (2012). Calcium imaging of multiple
770 neurons in freely behaving *C. elegans*. *J Neurosci Methods* **206**, 78-82.
- 771 Zou, W., Cheng, H., Li, S., Yue, X., Xue, Y., Chen, S., and Kang, L. (2017). Polymodal
772 Responses in *C. elegans* Phasmid Neurons Rely on Multiple Intracellular and
773 Intercellular Signaling Pathways. *Sci Rep* **7**, 42295.

774

775

776

777

778

779

780 **Figure Legends**

781 **Figure 1. Expression of *Psrx-97::mCherry* in ASH and PHB neuron:** (A) A cartoon
782 image showing the location of the amphid and phasmid neurons in *C. elegans*. (B)
783 Shows expression of the *Psrx-97::mCherry* transgenic construct in the whole animal.
784 (C) Shows the *srx-97* promoter (600 bp) expression in a single pair of amphid and
785 phasmid neurons. (D) shows the expression of the *srx-97* promoter (2 kb) in a pair of
786 amphid neurons and (E) phasmid neurons in *C. elegans*. (F) Indicates the expression of
787 *Psrb-6::GFP* and *Posm-10::GFP* in their respective neurons (indicated on the figure)
788 and their co-localization with *Psrx-97::mCherry* in the amphid ASH neurons (G)
789 Indicates the expression of *Posm-10::GFP* in its respective neurons (indicated on the
790 figure) and their co-localization with *Psrx-97::mCherry* in the phasmid PHB neuron. The
791 lower panel indicates a DIC image indicating the position of the PHA and PHB neurons
792 (H) Indicates the expression of *SRX-97::mCherry* in the cell bodies (dotted circles) and
793 *SRX-97* localization to the cilium tip of the ASH neurons (between the dotted circles in
794 the figure to the left).

795

796 **Figure 2. The *SRX-97* transmembrane domain and CRISPR/Cas9 generated**
797 **mutation of *srx-97*:** (A) The amino acid sequence showing the predicted seven
798 transmembrane domain of *SRX-97*. (B) The exonic structure of the *srx-97* gene with the
799 red line showing the CRISPR/Cas9 deletion obtained. The deletion encompasses the
800 gene from the 61st base pair to the 1895th base pair including part of the 3' UTR of the
801 gene. (C) Amplification of the chromosomal region showing the deletion of the *srx-97*
802 gene (2730 bp) using CRISPR/Cas9 compared to control wild-type (WT, 4566 bp) gene.
803 A 1 kb DNA ladder was used in the line marked Marker (M). Figure 2-1 is supporting
804 figure 2.

805

806 **Figure 3. Behavior of *srx-97* mutant animals towards water-soluble and volatile**
807 **chemicals:** (A) Graph showing the delay in avoidance response towards a dry spot of
808 2 M glycerol in WT, *srx-97* and *odr-3* mutant animals. The number of animals assayed
809 for each genotype are indicated at the base of each plot for panels A-D. (B) Graph
810 showing the delay in avoidance towards a dry spot of 0.1% SDS in WT, *srx-97* and *odr-3*
811 mutant animals. (C) Graph showing the delay in avoidance towards a dry spot of 10
812 mM CuSO_4 in WT, *srx-97* and *odr-3* mutant animals. (D) Graph showing the percentage
813 of avoidance upon nose touch stimuli of WT, *srx-97* and *glr-1* mutant animals. The
814 numbers at the base of graphs in A, B, C and D indicate the number of animals tested
815 for each genotype. (E) Graph indicating the negative chemotaxis indices of WT, *srx-97*
816 and *odr-3* mutant animals toward the repellent octanol. The assay was done in
817 triplicates over multiple days for all chemotaxis assays. Each dot indicates an assay done
818 in triplicate for all graphs from E-H. (F) Chemotaxis indices towards high concentrations
819 (10^{-1}) of diacetyl (DA) and isoamyl alcohol (IAA). (G) Chemotaxis indices towards

820 multiple concentrations of benzaldehyde. (H) Chemotaxis indices towards high
821 concentrations of benzaldehyde in WT, *srx-97* and rescue strains of *srx-97*. This rescue
822 experiments used SRX-97 under its own promoter and under the *osm-10* promoter.
823 Animals that did not show expression of the arrays (NA or No Array) were used as
824 controls in these experiments. The error bars represent SEM and statistical significance
825 is represented as “ns” for not significant, “*” $p<0.05$, “**” $p<0.01$ and “****” $p<0.001$. The
826 numbers at the base of each graph from E to H indicates the total number of times the
827 experiment was performed with 50-150 animals used in each trial. Figure 3-1 is
828 supporting figure 3.

829

830 **Figure 4. Ablation of ASH neurons shows defects towards chemosensation to**
831 **benzaldehyde:** (A) An illustration of the design of the plates used for analyzing the
832 chemotaxis frequency of *C. elegans* along with the formula used for this calculation.
833 Each sector (a,b,c and d) is 1 cm in width. (B) Graph of chemotaxis frequencies of WT,
834 *srx-97*, the *srx-97* rescue line and a control *odr-3* mutant line to a high concentration of
835 benzaldehyde. The assay was performed in triplicate over multiple days with each dot
836 indicating an assay done in triplicate. The numbers at the base of each plot indicate the
837 number of times the experiment was performed with each genotype. (C) Graph plotting
838 the delay in response of animals towards a high benzaldehyde concentration. The
839 animals used in this experiment have undergone mock ablation or ASH ablation in WT
840 or *srx-97* mutant backgrounds. Each dot indicates a response from a single animal.
841 About 25 mock ablated animals and ASH ablated animals in WT and *srx-97* mutant
842 background were analyzed for this experiment over multiple days. The error bars
843 represent SEM and statistical significance is represented as “ns” for not significant, “*”
844 $p<0.05$ and “****” $p<0.001$.

845

846 **Figure 5. The *srx-97* mutant phenotype is suppressed by other signaling mutants**
847 **that appear to function downstream of SRX-97:** (A) Chemotaxis indices with respect
848 to high concentration of benzaldehyde in WT, *srx-97*, *osm-9*, *tax-2*, *tax-4* and *gpc-1*
849 mutants along with analysis of each mutant in the *srx-97* background. (B) Chemotaxis
850 indices with respect to high concentration of benzaldehyde in WT, *srx-97*, *odr-3* and *srx-*
851 *97; odr-3* mutants. This graph also indicates chemotaxis indices with respect to
852 benzaldehyde upon ablation of the AWC neuron (AWC(-)) in WT, *srx-97* and *odr-3*
853 mutants. The assays were performed in triplicate over multiple days. Each dot in both
854 plots A and B indicates an assay done in. The numbers at the base of each graph in A
855 and B indicate the total number of times the experiment was performed with each
856 genotype. The error bars represent SEM and statistical significance is represented as
857 “ns” for not significant, “*” $p<0.05$, “**” $p<0.01$ and “****” $p<0.001$.

858

859

860 **Extended Figures**

861 **Figure 2-1. SRX-97 is not required for aldicarb-induced paralysis in *C. elegans*:** (A)
862 Graph of *C. elegans* paralyzing on aldicarb performed with WT and *srx-97* mutant
863 animals. The assay was performed over a course of two hours and the percentage of
864 animals paralyzed was plotted every 10 min. There was no significant difference
865 between the percentage of animals paralyzed at any given time point in *srx-97* when
866 compared to the WT control animals. The experiment was performed in triplicate with
867 20-25 animals were assayed per genotype for each experiment.

868

869 **Figure 3-1. Overexpressing SRX-97 does not affect behavior of the animals**
870 **towards benzaldehyde:** (A) Schematic of a plate showing four quadrants. The two
871 opposite quadrants shows the test spots (termed T) and the control spots (termed C),
872 50-150 animals are added in the central spot and the chemotaxis index for volatile
873 chemicals calculate by using the indicated formula. (B) the chemotaxis indices of the
874 WT, *srx-97* mutant animals and overexpression lines expressing the *srx-97* gene under
875 its endogenous promoter or the *osm-10* promoter in WT background. (C) The
876 chemotaxis indices of the WT, *srx-97* mutant animals and the rescue lines expressing
877 *srx-97* gene tagged with mCherry under its endogenous promoter in *srx-97* mutant
878 background. The rescue line shows nonsignificant defects when compared with WT
879 controls or *srx-97* mutant animals. The assays in B and C were done in triplicates over
880 multiple days. Each dot in the graphs B and C indicates an assay done in triplicate. The
881 error bars represent SEM and statistical significance is represented as “ns” for not
882 significant and “*” $p < 0.05$. The numbers at the base of each plot in B and C indicate the
883 number of times the experiment was performed with 50-150 *C. elegans* used in each
884 trial.

885

886

887

888

889

890

891

892 **Acknowledgments**

893 The authors are especially grateful to Yogesh Dahiya for help with making the *srx-97*
894 deletion strain. A number of strains were provided by CGC, which is funded by NIH
895 Office of Research Infrastructure Programs (P40 OD010440). The authors thank Ankit
896 Negi for routine work, Pratima Pandey and Umer Saleem Bhat for help with cloning and
897 the IISER Mohali Confocal facility for use of the confocal microscope. AG-R thanks
898 Harjot Kaur for the help with 2-Photon microscopy.

899 NYK thanks Council of Scientific and Industrial Research (CSIR)- University Grants
900 Commission (UGC) for a graduate fellowship and was also funded by a Department of
901 Science and Technology (DST)- Science and Engineering Research Board (SERB)
902 grant to KB. SB was funded by a KVPY fellowship for undergraduate students. KB was
903 an Intermediate Fellow of the India Alliance (IA) and thanks the Alliance for funding
904 support. KB also thanks DST- SERB and DBT for funding support.

905

906 **Funding**

907 This work was supported by the DBT/Wellcome Trust India Alliance fellowships [grant
908 numbers IA/S/19/2/504649 and IA/I/12/1/500516] awarded to KB and partially supported
909 by DBT, MHRD–STARS and DST–SERB grants [BT/PR24038/BRB/10/1693/2018,
910 STARS/APR2019/BS/454/FS and SERB/F/7047] as well as a DBT-IISc partnership
911 grant to KB. AG-R lab is supported by the NBRC core fund from the Department of
912 Biotechnology and a DBT/Wellcome Trust India Alliance fellowship [grant number
913 IA/I/13/1/500874] awarded to AG-R.

914 **Author Contributions**

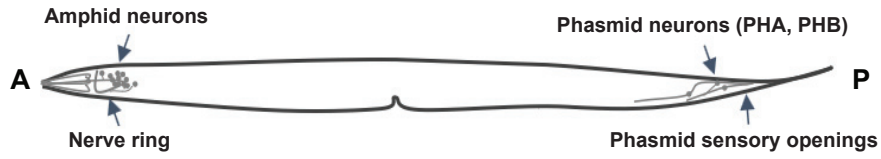
915 NYK designed, performed, analyzed all the experiments and wrote the manuscript. SB
916 helped with designing and performing experiments. SK and AG-R helped with performing
917 the ablation experiments and editing the manuscript. KB supervised the experiments,
918 helped with experimental design and data interpretation and edited the manuscript.

919 The authors declare no conflict of interest.

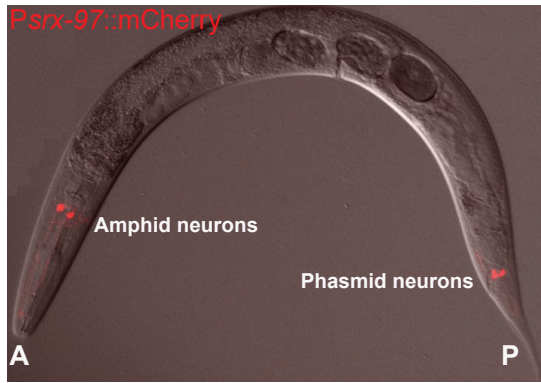
920

Figure 1

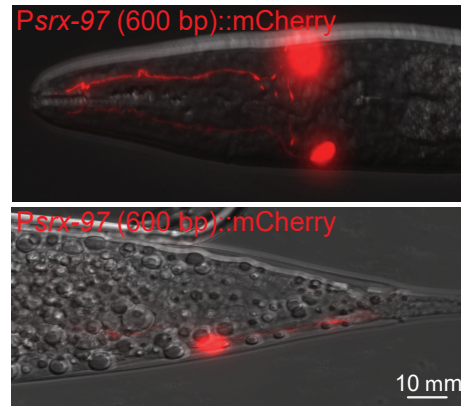
A



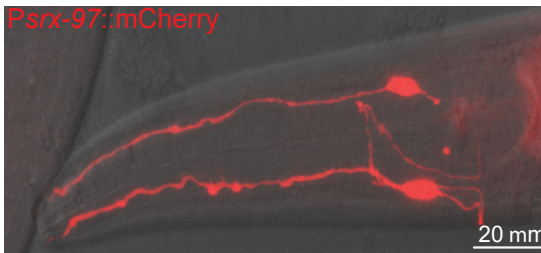
B



C



D



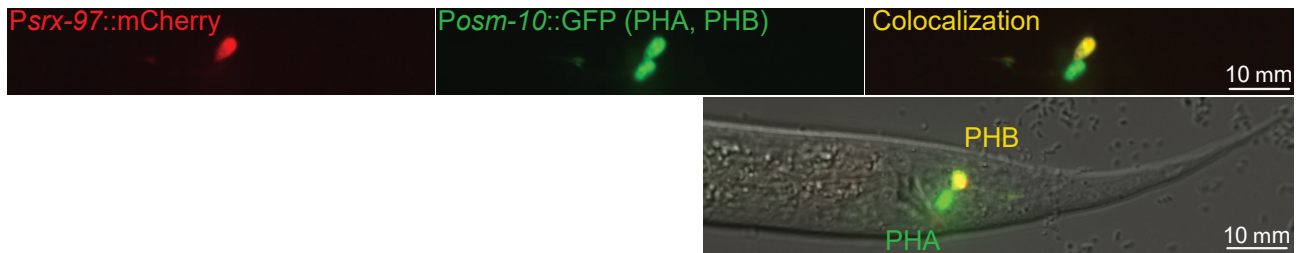
E



F



G



H

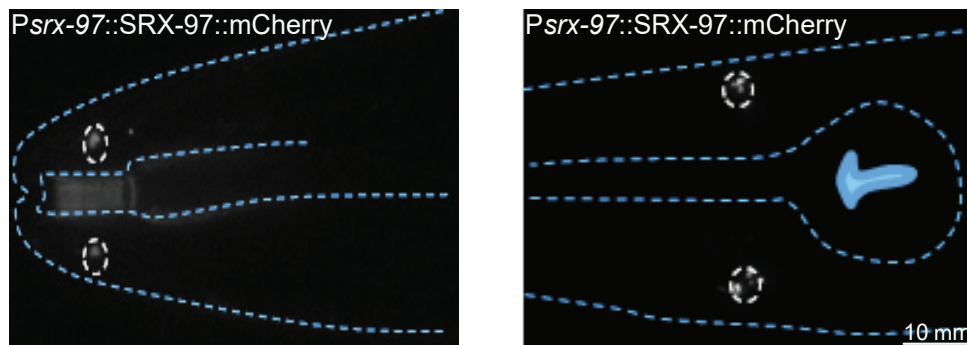


Figure 2

A

```

MSLSNWTLEQIWIEDSRPEDIATPLMTITAGVFMII
ASAFGIFINILVLRHFIKNSMSSFYLMCSSKTVSNS
IILFCYLIFNGPVSVGRSYYGPEFMMLLNQMAAY
GIYVQGPMTQVCISFNRFMVIYFVSLAKRKSGRL
ATITALCTCWTISFIVTIAGIKNCTNIFNYEILTWD
NLDPCVDILADMYWIGFLAIIISNTFNVVAVKLIIV
SASPHMDSTASKRRKRRTSRNLFQSCFDWVYLID
TINSMYIYSWFSDILWQFFFTIFS NLMVHVTDGCI
MLFFNYEGKKKTLTLTLNNVKREVTVLTVTF
    
```

B



C

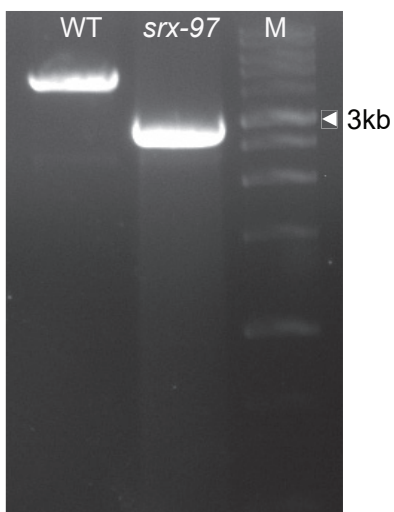


Figure 3

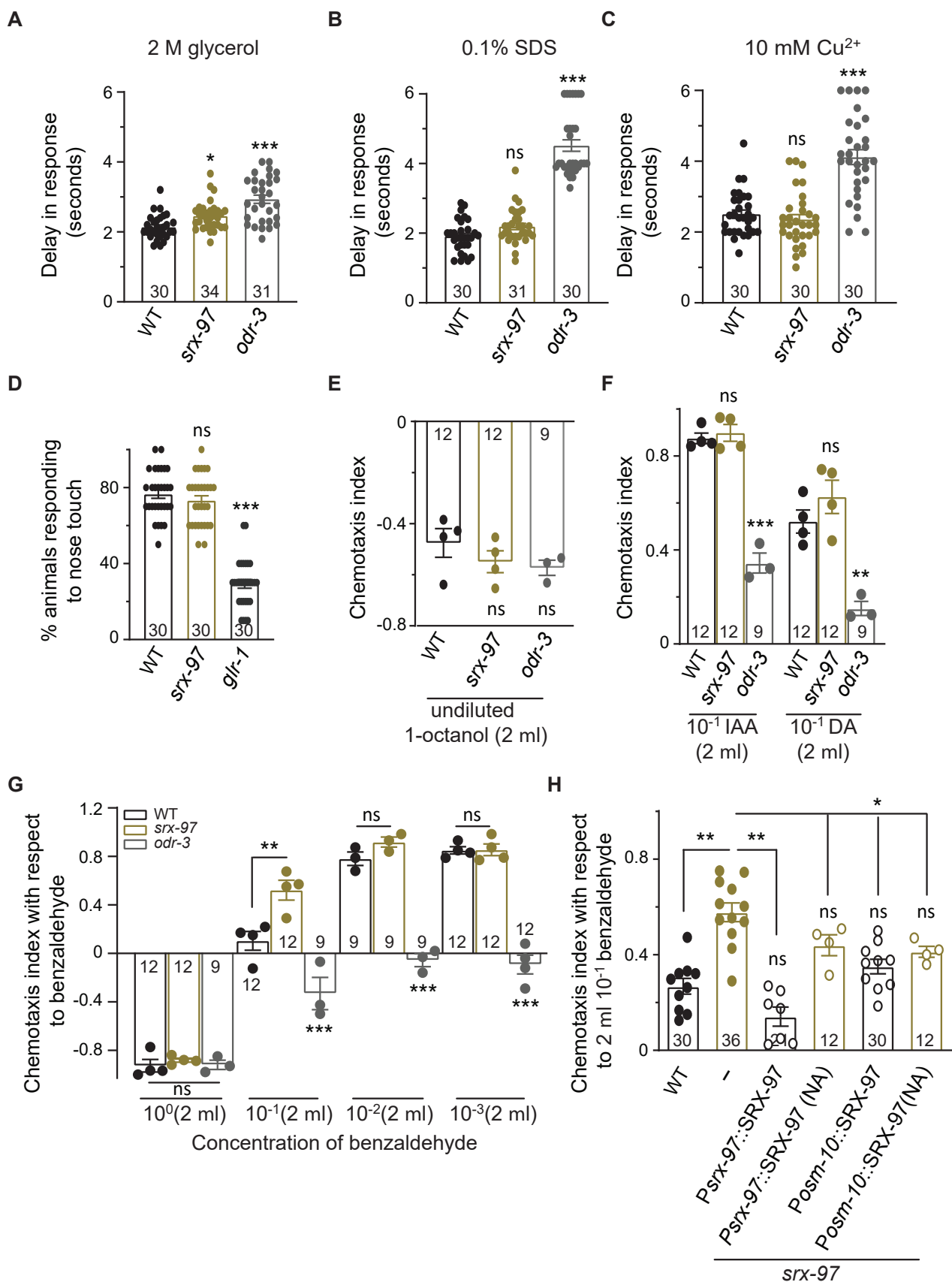
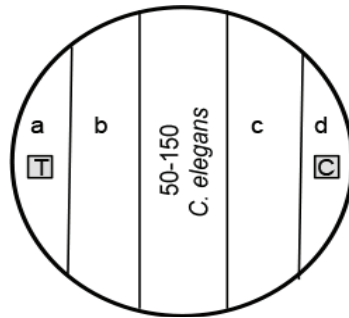


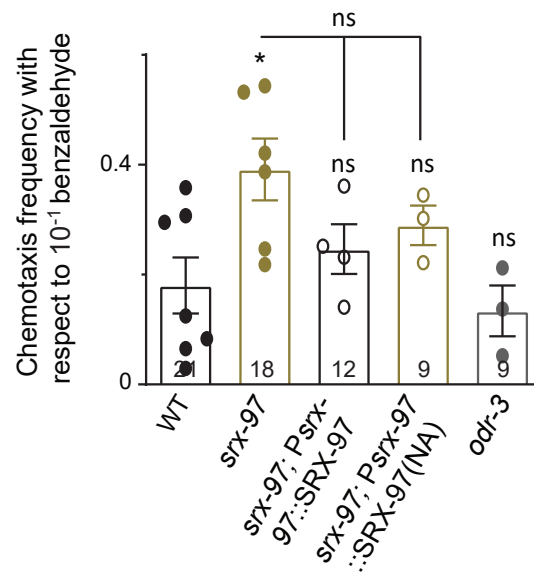
Figure 4

A



Chemotaxis frequency = $\frac{[\text{No. of } C. \text{ elegans in (a+b)} - \text{No. of } C. \text{ elegans in (c+d)}]}{\text{Total number of animals on plate}}$

B



C

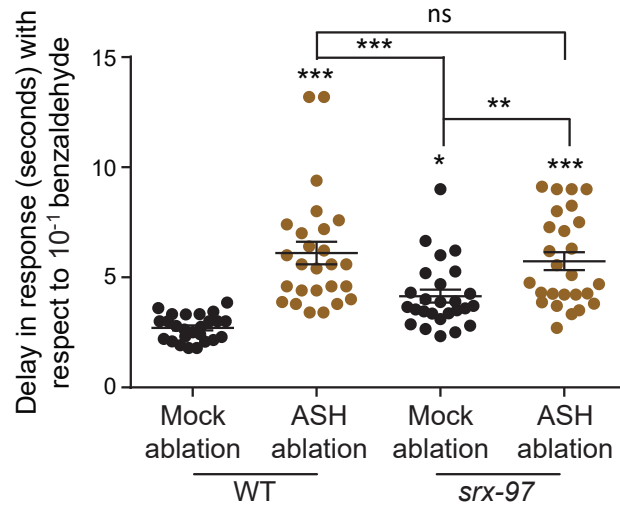
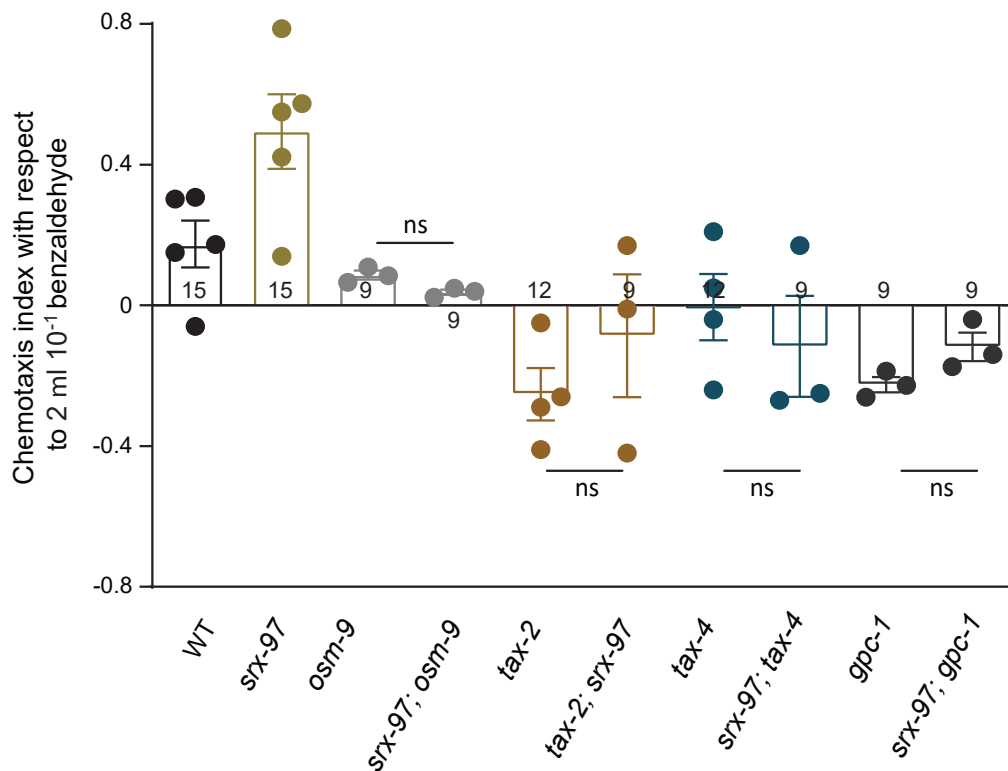


Figure 5

A



B

